



## **SEISMIC VULNERABILITY ASSESSMENT OF A RAILWAY OVERBRIDGE USING FRAGILITY CURVES**

Shinoj A. Kurian<sup>1</sup>, Sajal K. Deb<sup>2</sup> and Anjan Dutta<sup>2</sup>

### **ABSTRACT**

The main objective of this paper is to develop the fragility curves for typical a railway overbridge by analytical approach. In this study, a sample three span, two lane railway overbridge, situated in a highly seismic region in the country, is considered for development of fragility curve for seismic vulnerability assessment. Capacity of the bridge has been determined by static nonlinear analysis (Pushover analysis). The damage parameters of the bridge were obtained by performing nonlinear time history analysis for different prescribed ground motion histories recorded in the past earthquakes. The fragility curves for the overbridge piers have been constructed assuming a lognormal distribution. The influence of modeling aspects of the overbridge structure on fragility curves has been investigated by considering two different structural models for the response analysis. It is observed that that the fragility curves are more sensitive to the structural modeling for higher damage level.

Keywords: Seismic Vulnerability, Fragility Curve, Bridge, Damage Level

### **INTRODUCTION**

Railway overbridges (ROB), like other types of bridges, are the life-line structures and are the critical components of the transportation systems. About 500 bridges have been damaged in 26th January 2001 Bhuj earthquake alone. Most of the bridges suffered severe damage or collapse due to failure of their piers, although the bridge decks were undamaged due to high in-plane stiffness. Therefore, it is important to develop measures to quantify the associated seismic risk and to predict the possible damages that can be experienced by the ROB structure under seismic events. With this risk quantified, rational decisions can be made as to whether the ROB / bridge should be retrofitted or replaced, or to accept the risk and leave the bridge in the existing state.

Seismic vulnerability assessment and development of fragility curves for existing bridges are getting increased attention among the researchers in the recent years. Fragility curves of bridges can be developed empirically as well as analytically. Empirical fragility curves are usually developed based on the damage reports from past earthquakes. Since earthquake damage data are very scarce in developing countries like India, analytical development of fragility is the only feasible approach of development of fragility curve. Analytical fragility curves are developed from seismic response analysis of bridges, and regression analysis of simulated response data to establish the probabilistic characteristics of structural demand as a function a ground motion parameter. Mander and Basoz (1999) have presented the theory of fragility curves for highway bridges. The damage states were

---

1. Post Graduate Student, Department of Civil Engineering, IIT Guwahati, Pin – 781 039, INDIA, shinoj@iitg.ernet.in  
2. Associate Professor, Department of Civil Engineering, IIT Guwahati, Pin – 781 039, INDIA, skdeb@iitg.ernet.in

numerically quantified by Ghobarah *et. al.* (1997) from the dynamic responses of the bridges under various levels of ground excitation. Hawang *et. al.*(2001) described detailed procedure for analytical development of fragility curves. Karim and Yamazaki (2001) observed that special care should be taken in selecting structure model and input motions for analytical development of fragility curves. Karim and Yamazaki (2003) have studied the influence of ground motion on fragility curves and proposed a simplified method of its development for certain class of bridges in Japan.

In this study, procedure for obtaining force-displacement behaviour of typical ROB piers by static nonlinear analysis (pushover analysis) has been outlined. Analytical method for development of fragility curves based on numerical simulation of seismic response of ROB subjected to prescribed earthquake excitations and regression analysis of simulated response are presented. Finally, influence of structural modeling on analytically developed fragility curves has been investigated.

## DESCRIPTION AND MODELING OF THE ROB

In the present study a sample ROB connecting IIT Guwahati campus and NH 31 has been considered for development of fragility curves for vulnerability assessment. The ROB consists of three simply supported spans, with two end spans of length 22.5 m and middle span of length 39 m. The superstructures, consisting of pre-stressed concrete longitudinal girders, cross beams and deck slab, are supported on two R.C. piers and abutments. Piers are of 6.67m in height and supported on the pile foundation. Type of soil can be categorized as medium as per IS 1893 (Part-I), 2002. Photograph of the ROB is shown in Fig.1. Two different structural models are considered in order to study the influence of structural modeling on the analytically developed fragility curves.



FIG. 1 Photograph of the sample ROB

### Lumped Mass Model

For the straight bridges with large number of equal spans and piers of equal height, with all piers exposed to the same coherent earthquake ground motion perpendicular to the bridge axis, simple lumped mass idealization is generally considered to be reasonable. Priestly *et. al.* (1996) observed that the response of the piers to be same as the response of overall bridge and suggested that a bridge can be represented by a single column with tributary mass from the two adjacent half spans of the superstructure. The structural analysis program SAP 2000 nonlinear (version 9.1) has been used to carry out the dynamic response analysis. Fig.2 shows the lumped mass idealized model of the sample ROB. The superstructure and ROB pier mass have been modeled with two mass idealization in which the mass from the superstructure ( $M_1$ ) is lumped at the mass centroid of the deck and mass from the pier ( $M_2$ ) is lumped at the centroid of the pier cap. The pier is modeled by nonlinear link element whose nonlinear properties are determined by push over analysis. Both the masses are connected by massless rigid link elements and the additional flexibility caused by the formation of plastic hinges at bottom of the pier has been modeled by providing yield penetration length with additional nodes.

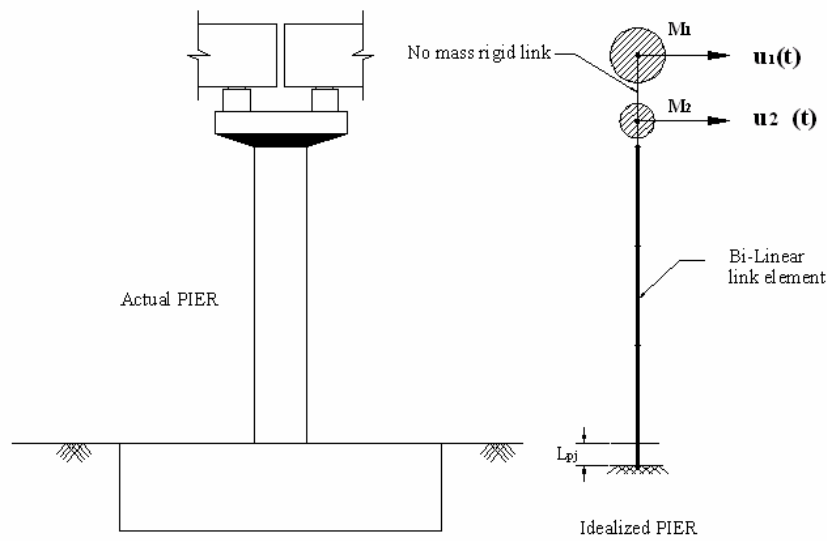


Fig.2 Lumped mass model

### Distributed Mass Model

The bridge superstructure can be considered as linear due to its high in plane stiffness. To investigate the influence of the mass distribution along the deck of the model on final fragility curves, the superstructure has been modeled by 3D beam elements with nodes, where the cross beams are intersecting the girder. Fig.3 shows the finite element model for the entire bridge system and the details of pier element is also shown inset. The mass of the superstructure is calculated and lumped at nodal points along the span. The piers have also been discretized to several elements to capture all the important modes of vibration. The connections between superstructure and piers or abutments have been modeled by using appropriate body constraints.

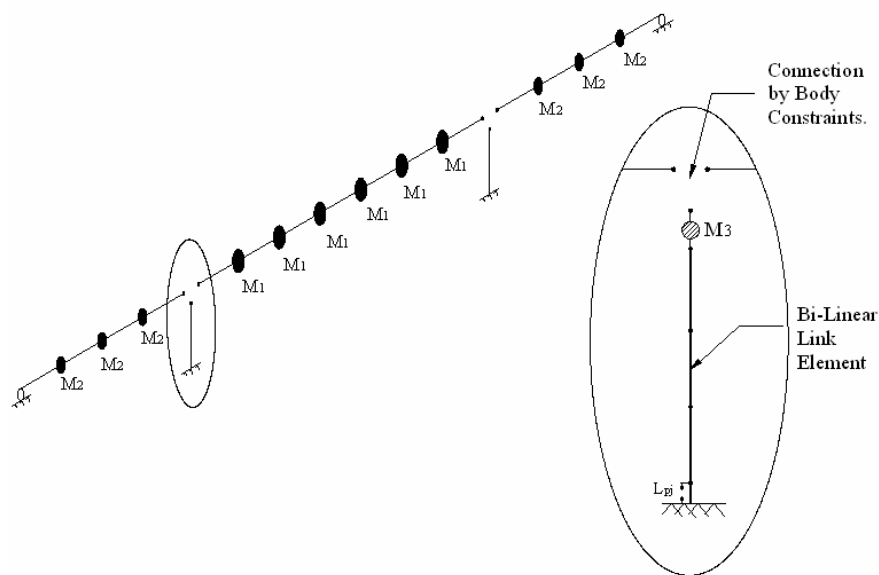


Fig.3 Distributed mass model

## DYNAMIC BRIDGE CHARACTERISTICS

Modal properties have been determined using Ritz vectors. The fundamental mode for both models are in the transverse direction with time periods of 1.3195 s and 1.2632 s for lumped mass model and distributed mass model respectively. Observation of basic modal properties of the ROB presented in the Table 1 and Table 2 show that effective modal mass participation of more than 99 % in both directions for lumped mass model is resulted in just three modes, while for distributed mass model, nine modes are needed to achieve 99 % and above mass participation. It appears that the distribution of mass increased the contribution of higher modes in the response of the bridge structure. The response of both the models of ROB subjected to NE India earthquake, 1988 with normalized PGA of 0.5g is shown in the Fig.4. The Fig.4 shows the difference between the responses of the two models as obtained from nonlinear time history analysis.

Table 1. Modal Properties of Lumped Mass Model

| Mode | Period in sec. | % of Mass participation |            |
|------|----------------|-------------------------|------------|
|      |                | Longitudinal            | Transverse |
| 1    | 1.3195         | 0                       | 84.69      |
| 2    | 1.0338         | 99.99                   | 0          |
| 3    | 0.5123         | 0                       | 15.31      |

Table 2. Modal Properties of Distributed Mass Model

| Mode | Period in sec. | % of Mass participation |            |
|------|----------------|-------------------------|------------|
|      |                | Longitudinal            | Transverse |
| 1    | 1.2632         | 0                       | 89.19      |
| 2    | 1.1707         | 99.99                   | 0          |
| 4    | 0.0222         | 0                       | 3.10       |
| 6    | 0.0082         | 0                       | 5.05       |
| 9    | 0.0023         | 0                       | 1.23       |

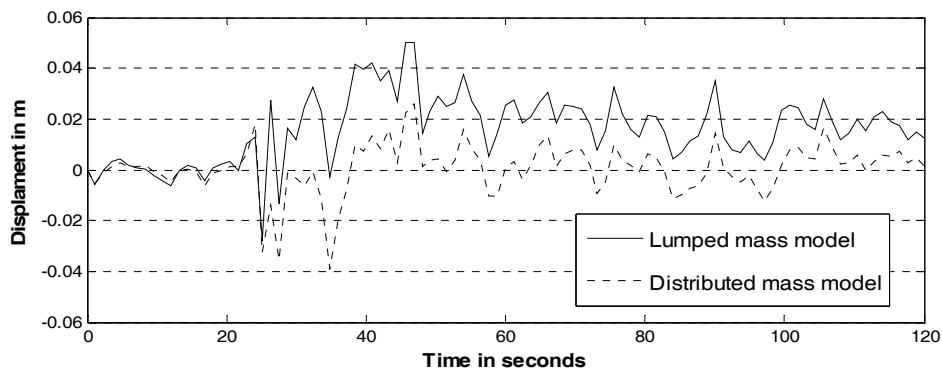


Fig.4 Comparison of response of both the models to NE India Earthquake, 1988

## STATIC NONLINEAR ANALYSIS (PUSH OVER ANALYSIS)

Static nonlinear analysis is carried out to obtain force displacement relationship at the top of the ROB pier. Priestley *et al.* (1996) observed that shear deformations can become significant in comparison with flexural deformation in squat piers, where the clear pier height is no longer significantly larger than the pier depth. In such cases, concentration of shear stress in pier may result the propagation of cracks and can affect the capacity of the structure. The capacity curve or force displacement relationship at the top of the ROB pier has been developed considering contribution of both flexural and shear deformation [Betz and Collins (2000)]. In this approach, the pier is divided into several slices along the height and sectional analysis is carried out to obtain moment-curvature and shear-shear strain relationship for each slices of the pier. Fig.5 and Fig.6 show the moment-curvature and shear-shear strain relationship at the base of the sample ROB pier. These relationships have been used for development of force displacement relationship at the top of the ROB pier as shown in Fig.7.

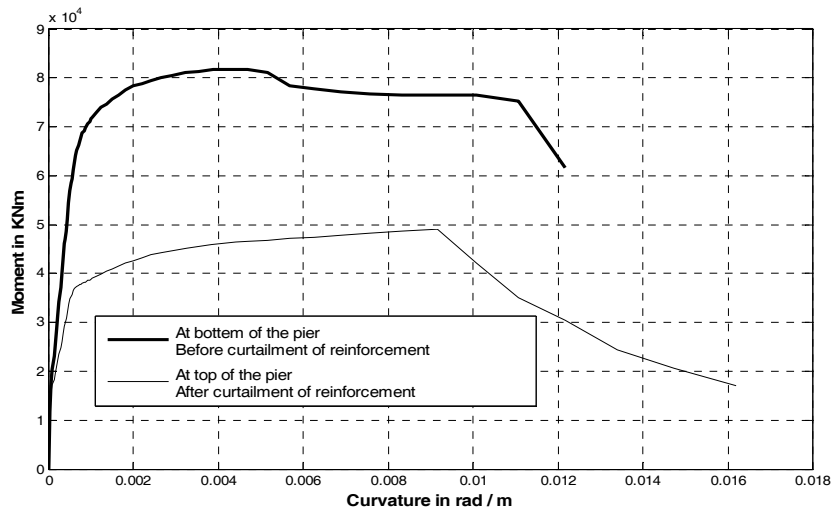


Fig.5 Moment-curvature relationship

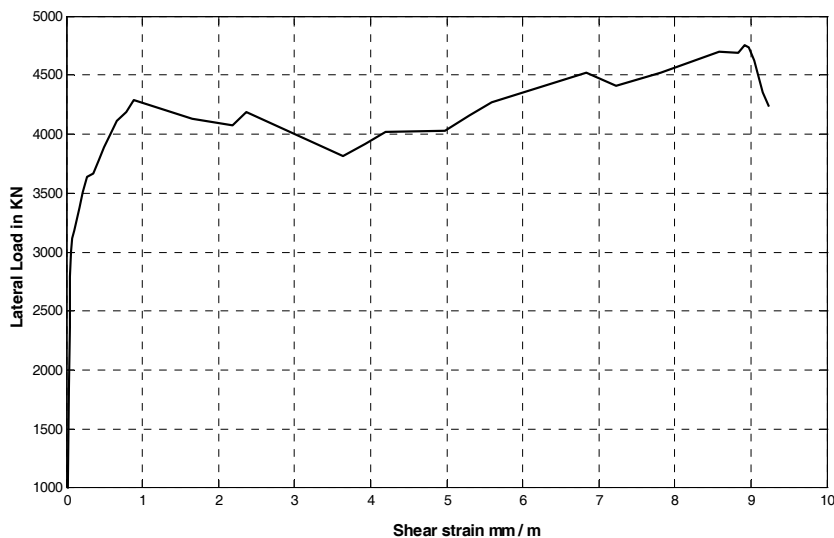


Fig.6 Shear-shear strain relationship

Fig.7 shows the load displacement relationship of the pier at initial yield level developed by push over analysis. On the basis of bilinear idealization of load displacement relationship, the yield force and yield displacement has been observed as 4500 KN and 3.7 mm respectively. These yield parameters have been used for nonlinear dynamic analysis of ROB subjected to earthquake excitations for the

assessment of ductility demand. Ultimate displacement ductility based on static nonlinear analysis has been observed to be 6.6 considering ultimate displacement as 0.4 percent of clear pier height.

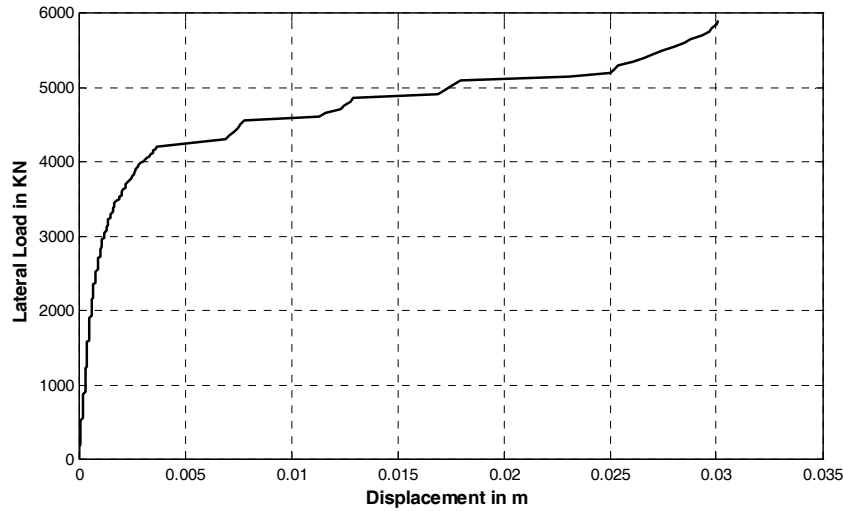


Fig.7 Lateral load displacement relationship at the pier top

### FRAGILITY CURVES

The fragility functions explicitly express the probability of meeting or exceeding the specific damage limit state for a specific intensity of seismic excitation. In this study, fragility curves are developed analytically with respect to peak ground acceleration (PGA) for seismic damage assessment of the sample ROB, because PGA is a commonly used parameter to express the severity of the earthquake. Ten strong motion data are selected for this analysis based on their characteristics. The selected ground motions are further normalized into different PGA levels from 0.1g to 1.5g to get wide ranges of ground motion records.

The displacement ductility and cumulative energy ductility have been determined from results of nonlinear dynamic analysis based on bilinear force displacement idealization using SAP 2000 nonlinear programme. *Ultimate ductility* ( $\mu_u$ ), which is defined as the ratio of maximum displacement to the yield displacement, has been obtained from static nonlinear analysis. *Cumulative energy ductility* ( $\mu_h$ ) is evaluated as the ratio of hysteretic energy dissipated during dynamic excitation to the energy at yield point as obtained from static nonlinear analysis. Further, *Displacement ductility* ( $\mu_d$ ) is also evaluated as the ratio of maximum displacement at the top of the pier obtained by the dynamic analysis to the displacement at the yield obtained from static analysis. Once these parameters are determined, the damage index (*DI*) of the structure can be quantified by the following relation given by Park and Ang (1985):

$$DI = \frac{\mu_d + \beta \cdot \mu_h}{\mu_u} \quad (1)$$

where,  $\beta$  = Cyclic loading factor taken as 0.15.

The damage levels in the range *no damage* to *complete damage* are defined from damage indices. The limit state of each damage level as proposed by Ghobarah *et. al.*<sup>2</sup> has been used in this study. Ranges of damage indices for different damage level have been presented in Table 3.

The damage ratio is defined as the ratio of the frequency of damage index for a particular PGA level to the total number of earthquake ground motions considered. The frequency of each level of damage can

be determined from the computed dynamic response and then the damage ratio is calculated. The damage ratio for each damage level are plotted on a lognormal paper with respect to logarithmic values of ground motion parameter (PGA) for determination of the parameters of fragility curves such as mean and standard deviation. These parameters can be obtained by least-square method of linear regression analysis using lognormal paper. When the parameters of the fragility functions have been evaluated, the fragility curves for different damage states can be plotted assuming lognormal distribution. Mean ( $\lambda_x$ ) and standard deviation ( $\xi_x$ ) for logarithm of PGA for different damage level are furnished in Table 4.

Table.3 Damage limit states for different damage levels

| Damage Index, DI      | Damage Level | Definition              |
|-----------------------|--------------|-------------------------|
| $0.00 < DI \leq 0.14$ | I            | <i>No Damage</i>        |
| $0.14 < DI \leq 0.40$ | II           | <i>Slight Damage</i>    |
| $0.40 < DI \leq 0.60$ | III          | <i>Moderate Damage</i>  |
| $0.60 < DI < 1.0$     | IV           | <i>Extensive Damage</i> |
| $1.00 \leq DI$        | V            | <i>Complete Damage</i>  |

Table.4 Mean and standard deviation of  $\ln(PGA)$

| Damage Level | Lumped mass model |         | Distributed mass model |         |
|--------------|-------------------|---------|------------------------|---------|
|              | $\lambda_x$       | $\xi_x$ | $\lambda_x$            | $\xi_x$ |
| I            | 7.546             | 0.5520  | 7.582                  | 0.5310  |
| II           | 7.987             | 0.7365  | 8.218                  | 0.8480  |
| III          | 8.325             | 0.6020  | 8.615                  | 0.6350  |
| IV           | 8.728             | 0.5680  | 8.823                  | 0.7140  |
| V            | 8.920             | 0.5430  | 9.053                  | 0.6405  |

Fragility curves are constructed with respect to PGA. The damage ratio for each damage level in each excitation level is obtained by calibrating the damage index using Table -3. Based on these data, fragility curves for the ROB piers are constructed assuming a lognormal distribution. For the cumulative probability  $P(\geq R)$  of occurrence of the damage equal or higher than level  $R$  is given as

$$P(\geq R) = \phi \left[ \frac{\ln X - \lambda_x}{\xi_x} \right] \quad (2)$$

where,  $\phi$  is the standard normal probability distribution,  $\lambda_x$  and  $\xi_x$  are the mean and standard deviation respectively of  $\ln X$  and  $X$  is the peak ground acceleration.

Two parameters of the distribution (i.e.  $\lambda_x$  and  $\xi_x$ ) obtained by the least-squares method on a lognormal probability paper are provided in Table-4. Finally, these two parameters are used to construct the fragility curves of the ROB pier due to the earthquake events.

## RESULTS AND DISCUSSION

The analytical fragility curves for all the damage levels have been developed using the parameters obtained from the linear regression analysis of damage data. It is observed from Table 4 that both mean and standard deviation for logarithm of PGA ( $\lambda_x$  and  $\xi_x$ ) increases with damage level. Fig.8 and Fig.9 show the analytical fragility curve for the sample ROB obtained from lumped mass model and distributed mass model respectively. It is observed that the slopes of the fragility curves with lower damage level are steeper compared to the same for fragility curve for higher damage levels for any level of PGA. This indicates that the cumulative probability of exceeding lower damage levels is very high within a small span of PGA, while the cumulative probability of exceeding higher damage levels increases gradually with the increase in PGA levels.

Comparison of analytical fragility curves obtained using the lumped mass model and distributed mass model have been made to investigate the influence of structural modeling. It is evident that cumulative probability of exceeding damage level – II to V estimated on the basis of lumped mass idealization is on the higher side compared to that obtained on the basis of distributed mass idealization for any PGA level. Thus, the influence of structural modeling on fragility curves has been observed to be significant for higher damage levels.

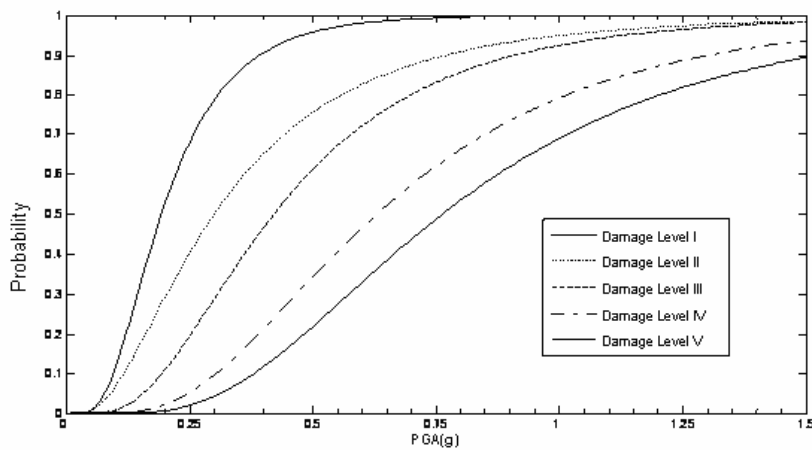


Fig.8 Fragility curves for ROB pier by lumped mass model

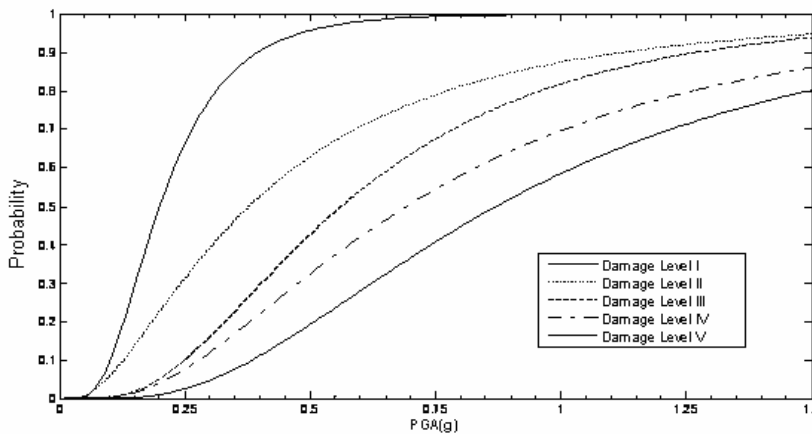


Fig.9 Fragility curve for ROB pier by distributed mass model

## CONCLUSION

In this study, static nonlinear analysis and nonlinear time history analysis have been used to determine the structural capacity and seismic demand respectively. An analytical method of construction of fragility curves for a sample ROB (located in zone – V) based on numerical simulations has been presented for assessment of seismic vulnerability. The influence of structural modeling on the fragility curves have also been investigated by considering two different analytical models. Comparison of analytical fragility curves obtained from lumped mass model and distributed mass model reveals that the influence of structural modeling is significant for higher damage levels.

## REFERENCES

- Betz, E.C. and Collins, M.P., (2000). *Response-2000, Software Program for Load-Deformation Response of Reinforced Concrete Section*.
- Ghobarah, A., Aly, N.M. and El-Attar, M., (1997). “Performance level criteria and evaluation”, Proceedings of the International Workshop on Seismic Design Methodologies for the next Generation of Codes. Balkema: Rotterdam, pp 207–215.
- Hwang H., Jing, B.L, and Chiu, Y., (2001). *Seismic Fragility Analysis of Highway Bridges*. Ref. No. MAEC RR-4, Center for Earthquake Research Information, Memphis.
- Karim, K.R. and Yamazaki, F., (2001). “Effect of earthquake ground motions on fragility curves of highway bridge piers based on numerical simulation”, *Earthquake Engineering and Structural dynamics*, 30, pp 1839-1856.
- Karim, K.R. and Yamazaki, F., (2003), “A simplified method of constructing fragility curves for highway bridges”, *Earthquake Engineering and Structural dynamics*, 32, pp 1603-1626.
- Mander, J.B. and Basoz, N., (1999). “Seismic fragility curves theory for highway bridges”, Proceedings of 5<sup>th</sup> U.S. Conference of Lifeline Earthquake Engg, ASCE, pp31-40.
- Park, Y.J. and Ang AH-S., (1985). “Seismic damage analysis of reinforced concrete buildings”, *Journal of Structural Engineering*, ASCE, 111(4), pp 740 –757.
- Priestley, M.J.N. and Calvi, G.M., (1996). *Seismic design and retrofit of bridges*, John Wiley & Sons Inc.